JOURNAL OF SOLID STATE CHEMISTRY 26, 389–396 (1978)

Crystal Structure and Antiferromagnetism of $EuSb_2$

F. HULLIGER

Laboratorium für Festkörperphysik ETH, CH–8093 Zürich, Switzerland

AND R. SCHMELCZER

Institut de Cristallographie, Université de Lausanne, CH–1015 Lausanne-Dorigny, Switzerland

Received March 13, 1978; in final form May 11, 1978

$EuSb_2$ crystallizes in the monoclinic $CaSb_2$ type of structure, space group $P2_1/m$, with $a = 4.768(2)$, $b = 4.299(2)$, $c = 8.970(3)$ Å, $\beta = 103.01(3)°$. The structural distortions of the $ZrSi_2$ type provide the Sb chains required for a Mooser–Pearson phase. $EuSb_2$ is antiferromagnetic below $T_N = 26.2°K$. From high-field magnetization measurements a weak anisotropy ($H_{anis.} \approx 6$ kOe at 1.5°K) is deduced. The spins are aligned perpendicular to the (001) planes. Susceptibility measurements between 30 and 1100°K gave no indication of a $Eu^{2+} \rightarrow Eu^{3+}$ transition.

Europium pnictides are rather badly investigated up to now, quite in contrast to the rocksalt-type chalcogenides. As part of our studies on europium antimonides we present here our structural and magnetic results on $EuSb_2$.

Experimental

$EuSb_2$ was synthesized by reacting the elements in a silica tube at 550 to 600°C followed by annealing at the upper temperature for 2 months. The reaction product contained three phases which are quite stable in air. The main part consisted of easily cleavable crystals with a chromium-like luster and turned out to have the desired composition $EuSb_2$. Elemental antimony was detected between the $EuSb_2$ lamellae. Irregular crystal aggregates with a slightly greyish tint were found to correspond to the formula Eu_2Sb_3. The structure of this phase is described elsewhere (*1*).

Structure Determination

Chemical reasoning and the lamellar habit of the $EuSb_2$ crystals led us to suspect isomorphism with $CaSb_2$ (*2*) and $SrSb_2$ (*3*) and this was confirmed by the crystallographic structure determination. The most appropriate crystal we could find for the structural analysis had a wedgelike form with approximate dimensions $0.1 \times 0.05 \times 0.03$ mm³. Intensities were collected on an automatic four-circle diffractometer Syntex $P\ 2_1$ with Nb-filtered Mo$K\alpha$ radiation ($\lambda_{MoK\bar{\alpha}} = 0.71069$ Å). Three independent sets of intensities were measured up to $2\theta = 70°$. The data were corrected for absorption ($\mu_{Mo} = 323$ cm^{-1}) by means of the Gaussian integration method. The absorption coefficients varied between 7 and 49. The error in the evaluation of the severe absorption along with the approximation in the crystal form may explain the rather high internal R value $R_I = 0.115$.

Reduction of the data resulted in 875 independent intensities of which 815 were larger

0022–4596/78/0264–0389$02.00/0

TABLE I

CRYSTAL DATA FOR $EuSb_2$, MONOCLINIC, $P2_1/m$ (No. 11), $Z = 2$[a]

	x	z	U_{11}	U_{22}	U_{33}	U_{12}	U_{13}	U_{23}[b]
Eu	0.4108(2)	0.2901(1)	0.0101(5)	0.0107(5)	0.0126(5)	0	0.0036(4)	0
Sb_I	0.8006(3)	0.0156(2)	0.0129(6)	0.0116(6)	0.0118(6)	0	0.0051(5)	0
Sb_{II}	0.0491(3)	0.6140(2)	0.0098(6)	0.0105(6)	0.0218(7)	0	0.0055(5)	0

[a] All atoms in 2(*e*): $\pm(x, \frac{1}{4}, z)$. At 25°C: $a = 4.768(2)$ Å, $b = 4.299(2)$ Å, $c = 8.970(3)$Å, $\beta = 103.01(3)°$, $V = 179.1$ Å^3.

[b] The anisotropic temperature factor is defined as $\exp(-2\pi^2 \sum h_i h_j a_i^* a_j^* U_{ij})$. Standard deviations of the last digits are given in parentheses.

than 3σ (I). In our structural analysis we made use of the X-Ray System 72 of Programs (*4*). Moreover, we used the atomic scattering factors calculated by Cromer and Mann (*5*) and the anomalous dispersion coefficients for Eu and Sb given by Cromer (*6*). The atomic positions of $SrSb_2$ (*3*) were taken as starting parameters in our refinement with a full-matrix least-squares procedure and anisotropic temperature coefficients. Our final R value was $R = \sum|\Delta F|/\sum|F_0| = 0.074$.

The lattice constants were calculated from a Guinier pattern taken with copper radiation ($\lambda_{CuK\alpha_1} = 1.54051$ Å), using silicon ($a_{295\,K} = 5.43054$ Å) as a standard. Our crystal data for $EuSb_2$ are listed in Table I[1] while the interatomic distances are collected in Table II.

TABLE II

INTERATOMIC DISTANCES IN $EuSb_2$[a, b]

Eu	2 Sb_{II}	at 3.315(3) Å
	2 Sb_{II}	at 3.319(3) Å
	1 Sb_I	at 3.361(3) Å
	1 Sb_I	at 3.402(3) Å
	2 Sb_I	at 3.451(3) Å
	1 Sb_{II}	at 3.698(3) Å
	1 Sb_{II}	at 3.704(3) Å
	2 Eu	at 4.252(3) Å
	2 Eu	at 4.299(2) Å
	2 Eu	at 4.768(2) Å
Sb_I	2 Sb_I	at 2.924(3) Å
	2 Sb_I	at 3.543(3) Å
	1 Eu	at 3.361(3) Å
	1 Eu	at 3.402(3) Å
	2 Eu	at 3.451(3) Å
	2 Sb_{II}	at 3.885(3) Å
Sb_{II}	2 Sb_{II}	at 2.931(3) Å
	2 Eu	at 3.315(3) Å
	2 Eu	at 3.319(3) Å
	1 Eu	at 3.698(3) Å
	1 Eu	at 3.704(3) Å
	2 Sb_I	at 3.885(3) Å

[a] The Sb–Sb–Sb angles within the chains are Sb_I–Sb_I–Sb_I 94.61(6)° and Sb_{II}–Sb_{II}–Sb_{II} 94.31(6)°.

[b] Standard deviations are given in parentheses.

Discussion of the Structure

The $EuSb_2$ structure is characterized by antimony zigzag chains running parallel to the *b*-axis (see Fig. 1, left-hand side). These infinite Sb_n^{-n} chains are held together by Eu^{2+} cations[2] which are bonded to 10 Sb^- neighbors belonging to four chains. The Sb–Sb distances are 2.924 and 2.931 Å, which is somewhat large but still may correspond to the expected single bonds, as in $CaSb_2$ (2.92 and 2.94 Å (*2*)), $SrSb_2$ (2.90 and 2.92 Å (*3*)), KSb (2.81 and 2.88 Å), and NaSb (2.85 and 2.86 Å), the variation being due to different effective charges. The angles within the Sb chains are

[1] A list of the measured and calculated structure factors may be obtained from the second author.

[2] Formally we use a simplifying black-and-white description (covalent bonds within the Sb chains, ionic bonds between Eu and Sb) which however does not imply a complete charge transfer. For a discussion of the bond lengths, etc., the covalent part of the Eu–Sb bonds has, of course, to be taken into account.

94.31 and 94.61°, similar to those met in $CaSb_2$ and $SrSb_2$. Sb_I and Sb_{II} are coordinated to 4 and 6 Eu atoms, respectively. In addition to the 2 Sb_I chain neighbors, Sb_I has two other Sb_I neighbors at a nonbonding distance of 3.543 Å. In the related compound $YbSb_2$, the corresponding 4 Sb_I neighbors are at equal distances. In Yb the divalent state is less stable than in Eu, and this is reflected also in the pnictides (see, e.g., Table 33.2 of Ref. *7*). According to susceptibility data (*8*) $YbSb_2$ contains about 2% Yb^{3+} below room temperature. It therefore looks as if the instability of the divalent state gave rise to the occurrence of the $ZrSi_2$ structure in $YbSb_2$ whereas the divalency of Eu required isomorphism with the Sr compound. Surprisingly, however, the unit-cell volume of $EuSb_2$ is almost 5% smaller than that given for $SrSb_2$ (*3*). As is demonstrated in Fig. 1 the $CaSb_2$-type structure of $EuSb_2$ is a distorted version of the $ZrSi_2$ type. The space group $P\ 2_1/m$ (No. 11) of $CaSb_2$ is a subgroup of the space group *Cmcm* (No. 63) of $ZrSi_2$ (9). In Fig. 1 both the $ZrSi_2$-derived cell for space group $C\ 2/m\ 2/c\ 2_1/m$ and the reduced cell for space group $P\ 1\ 2_1/m\ 1$ are indicated.

In the undistorted $ZrSi_2$ structure of $YbSb_2$ the Sb_I atoms form puckered square nets with metallic bonding. The $ZrSi_2$-type structure of $YbSb_2$ can in fact be built up by inserting these Sb_I square nets between the infinite trigonal-prism slabs of a CrB-type structure (see Fig. 1, right-hand). The actual distortions met in $CaSb_2$-type compounds represent one possibility of how to replace the four fractional Sb–Sb bonds by two single bonds. In fact, it is also the most adequate deformation since it makes all Sb atoms nearly equivalent. A similar deformation of the anion square net in

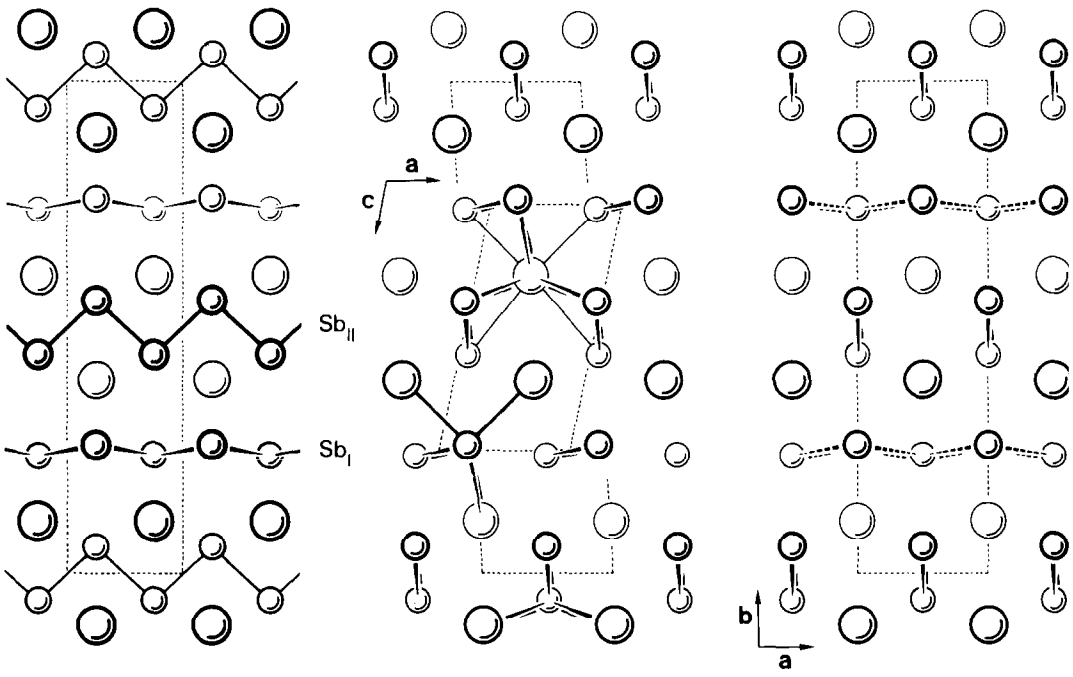

FIG. 1. The $CaSb_2$-type structure of $EuSb_2$ as derived from the $ZrSi_2$-type structure of $YbSb_2$. Eu: large spheres, Sb: small spheres. In the section perpendicular to the *a*-axis on the left-hand side, only the $ZrSi_2$-derived cell is indicated. All the anion–anion bonds are shown whereas Eu–Sb bonds are given only to visualize the three different coordinations.

the PbFCl structure leads to the monoclinic CeAsS structure (*10*). In both cases these distortions are necessary for bond saturation; i.e., only the compounds with the distorted structures are Mooser–Pearson phases[3] and hence nonmetallic (or semimetallic). We must however admit that we were unable to confirm the expected semiconductor properties of $EuSb_2$, but this failure—if it is not caused by partially trivalent Eu–may be due to admixed elementary antimony.

Deller and Eisenmann (*2*) stated that a great part of the $CaSb_2$ platelets were twinned. This probably indicates a high-temperature transition to the $ZrSi_2$ structure, i.e., a semiconductor → metal transition. In $EuSb_2$ such a transition might be coupled with a partial valence change of Eu (although in fact the valence-electron concentrations of $Eu^{2+}Sb_2$ and $ZrSi_2$ are the same, and moreover, an increase of the Eu^{3+} concentration is to be expected rather on lowering the temperature). Susceptibility measurements gave no indication of a valence transition up to 800°C; the Curie–Weiss law was perfectly obeyed. Even without any $Eu^{2+} \rightarrow Eu^{3+}$ (or rather $Eu^{3+} \rightarrow Eu^{2+}$) transition, the susceptibility increase due to the Pauli spin paramagnetism of the additional free carriers in a hypothetical $ZrSi_2$-type modification should amount to a few percents above 800°C. We have indeed observed a continuous increase above 830°C, reaching 2% at 870°C, the maximum temperature attained. But since afterwards our sample stuck to the quartz holder we doubt whether this deviation was reliable, although on cooling the susceptibility data were perfectly reproducible (possibly we were close to the melting point).

On the other hand, a complete valence transition can be expected to occur under high pressure and to lead to the $SmSb_2$ structure. This structure type contains half the anions in pairs and thus implies metallic properties as well.

[3] We use the term Mooser–Pearson phase for a compound which obeys the Mooser–Pearson bond rules (*11*), in order to honor the merit of E. Mooser and W. B. Pearson in the elucidation of the relationship between structure and electronic properties. In German papers polyanionic Mooser–Pearson phases like $EuSb_2$ are usually called Zintl phases (*2, 3, 12*).

Low-Temperature Magnetic Measurements

Contamination of our crystals with elementary antimony (as detected by electron-beam microanalyses) reduces somewhat the absolute accuracy of our data but the general magnetic behavior remains unaffected. Moreover, Eu^{2+} is an S-state ion, so that its magnetic moment is not affected by the crystal electric field. Assuming 100% divalency we have used the effective magneton number derived from susceptibility measurements in the paramagnetic range to calculate the effective Eu concentration.[4]

$EuSb_2$ turned out to be antiferromagnetic below a Néel temperature $T_N = 26.2$°K. Magnetization measurements (Fig. 2) revealed a weak anisotropy obviously connected with the layered crystal structure. In magnetic fields perpendicular to (001) the spins flop at $H_{flop} \approx 27$ kOe (1.5°K). From the pulsed-field data below 4.2°K we estimate an anisotropy field $H_{anis.} \approx 6$ kOe and an exchange field $H_{exch.} \approx 65$ kOe.

Since our definitions are adapted to the actual case it might be worthwhile to sketch the derivation of $H_{anis.}$ and $H_{exch.}$. If we denote by θ_A and θ_B the angles between the sublattice magnetizations M_A and M_B

[4] We cannot exclude a partial trivalency of Eu. However, if the observed moment reduction were exclusively due to Eu^{3+}, then it should probably not vary within the same batch. Instead of the theoretical value 7.94 μ_B we derived 7.69 μ_B from the Curie–Weiss straight line below room temperature obtained from a 15-mg crystal oriented with the (001) faces parallel to the applied field, 7.45 μ_B from a 30.5-mg crystal oriented perpendicular to the magnetic field, and 7.65 μ_B from the high-temperature measurements on a 45-mg crystal. An earlier measurement carried out ten years ago on a polycrystalline sample of 280 mg led to 8.05 μ_B (and $T_N = 26$°K, $\theta_p = -2$°K).

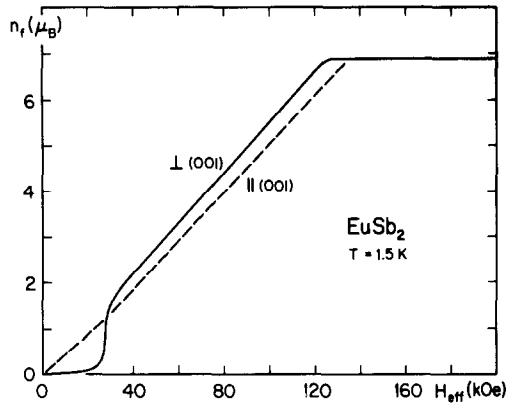

FIG. 2. Magnetization measurements at 1.5°K on $EuSb_2$ crystals oriented with the cleavage plane (001) parallel and perpendicular to the applied field. The magnetic moments are corrected so as to correspond to 100% Eu^{2+}.

(where M_A comprises the magnetic moments oriented in one direction and M_B those which in zero external field are oriented in opposite direction) and the easy axis, then for an external magnetic field H applied along or perpendicular to the easy axis the anisotropy energy $E_{\text{anis.}}$, the exchange energy $E_{\text{exch.}}$ and the Zeeman energy E_H are given by the following expressions (all per unit volume):

$$E_{\text{anis.}} = (K/2)(\sin^2\theta_A + \sin^2\theta_B),$$
$$E_{\text{exch.}} = -N\langle S\rangle^2\{\mathcal{J}_{\uparrow\uparrow} + \mathcal{J}_{\uparrow\downarrow}\cos(\theta_A - \theta_B)\},$$
$$E_{H\parallel} = -(N/2)\,g\mu_B\langle S\rangle H(\cos\theta_A + \cos\theta_B),$$
$$E_{H\perp} = -(N/2)\,g\mu_B\langle S\rangle H(\sin\theta_A + \sin\theta_B),$$

where K is the anisotropy constant for uniaxial anisotropy, $\langle S\rangle$ is the average spin value, $\mathcal{J}_{\uparrow\uparrow}$ is the exchange parameter for all neighbors with parallel and $\mathcal{J}_{\uparrow\downarrow}$ for antiparallel spin orientation, and N is the number of cations per unit volume. If we define an anisotropy field $H_{\text{anis.}}$ and an exchange field $H_{\text{exch.}}$ by

$$H_{\text{anis.}} = \frac{K}{(N/2)\,g\mu_B\langle S\rangle},$$

$$H_{\text{exch.}} = \frac{2|\mathcal{J}_{\uparrow\downarrow}|\langle S\rangle}{g\mu_B}.$$

($H_{\text{exch.}}$ contains only the antiferromagnetic part of the interactions) then minimizing of the energy expression leads to the usual formulas for the spin–flop field H_{flop} and the saturation fields $H^{\parallel}_{\text{sat.}}$ and $H^{\perp}_{\text{sat.}}$:

$$H_{\text{flop}} = (2H_{\text{exch.}}H_{\text{anis.}} - H^2_{\text{anis.}})^{1/2},$$
$$H^{\parallel}_{\text{sat.}} = 2H_{\text{exch.}} - H_{\text{anis.}},$$
$$H^{\perp}_{\text{sat.}} = 2H_{\text{exch.}} + H_{\text{anis.}}.$$

The difference between the antiferromagnetic susceptibilities in low magnetic field, $\chi(T_N)$ and $\chi_\perp(T \to 0)$ allows an independent determination of $H_{\text{anis.}}/H_{\text{exch.}}$ since $\chi(T_N)/\chi_\perp(0) = 1 + H_{\text{anis.}}/2H_{\text{exch.}}$. These data, however, are much more sensitive to a second magnetic phase or to imperfect orientation of the crystals. Within the expected accuracy our measurements on two different $EuSb_2$ crystals were in fair agreement with the expected value $\chi(T_N)/\chi_\perp(T \to 0) \approx 1.05$.

If we apply the molecular-field expressions which relate the paramagnetic Curie temperature θ_p and the ordering temperature T_N with the exchange parameters

$$k\theta_p = \tfrac{2}{3}\mathcal{J}_p\,S(S+1),$$
$$kT_N = \tfrac{2}{3}\mathcal{J}_{af}\,S(S+1),$$

where in our case $\mathcal{J}_p = \mathcal{J}_{\uparrow\uparrow} - \mathcal{J}_{\uparrow\downarrow} \approx 0$ and $\mathcal{J}_{af} = \mathcal{J}_{\uparrow\uparrow} - \mathcal{J}_{\uparrow\downarrow} = g\mu_B H_{\text{exch.}}/\langle S\rangle$ (see below), then the experimental value for $H_{\text{exch.}} = 65$ kOe leads to exactly the same value $T_N = 26.2$°K as derived from the $\chi(T, H \to 0)$ maxima.

The variation of the Néel temperature T_N with the effective field (applied field corrected for demagnetization) is shown in Fig. 3. From the magnetization curves $M(H)$ we can deduce that the magnetic moments are oriented perpendicular to the (001) planes. The cation sublattice of $EuSb_2$ is made up of double layers parallel to (001) (these are the trigonal-prism slabs of the CrB-like part of the structure). The width of these double layers is 3.669 Å, while their distance is 5.071 Å. The $EuSb_2$ structure allows for different magnetic arrangements: (a) each (001) plane could be

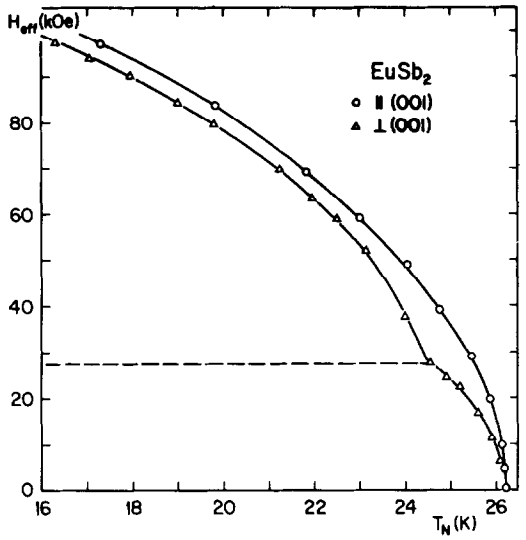

FIG. 3. Field dependence of the Néel temperature T_N of $EuSb_2$ (maxima of the $M(T)$ curves). The broken line indicates the spin–flop transition.

antiferromagnetic in itself, though this is not very probable, (b) simple ferromagnetic (001) layers can be stacked antiferromagnetically +− +−, (c) ferromagnetic double layers may be antiferromagnetically coupled. This can be realized either by ferromagnetic intra-slab (++ −−) or by ferromagnetic interslab coupling (+− −+).

In Fig. 4 we have indicated some possible superexchange paths. Within a coordination sphere of 7 Å Eu has 18 Eu neighbors. The two closest Eu neighbors are those at 4.252 Å within the Eu double layer along the zigzag chain (60.72°) running in b-direction. The corresponding exchange interaction ($\mathcal{J}_1$) is either "direct" via d-orbitals or indirect via ~ right-angle superexchange (1 in Fig. 4, Eu–Sb–Eu = 74.28° (α) and 74.39° (β). The next nearest neighbors are those along the b-axis

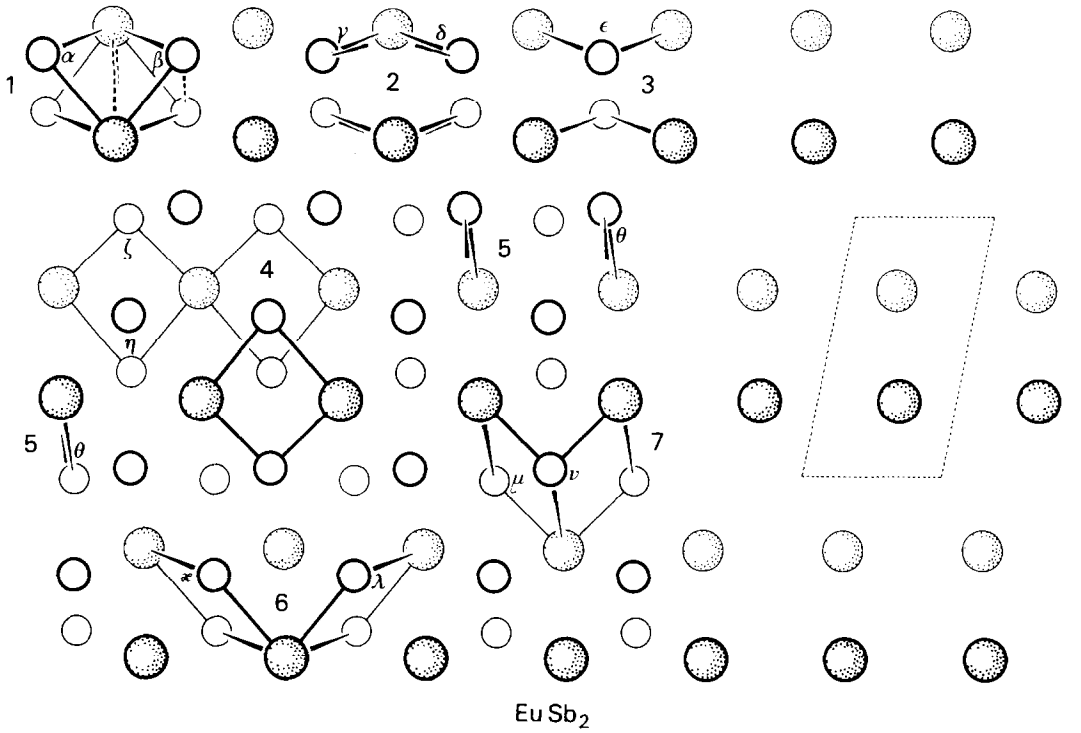

FIG. 4. Bonds which mediate exchange in the $EuSb_2$ structure, projected onto (010). Eu: large stippled spheres. Sb: small empty spheres. The faint circles indicate atoms at $y = \frac{1}{4}$, the fat ones are at $y = \frac{3}{4}$. The antimony atoms are omitted on the right part in order to emphasize the Eu double layers. The Eu–Sb–Eu angles (°) are: $\alpha = 74.29$; $\beta = 74.42$; $\gamma = 80.71$; $\delta = 80.83$; $\varepsilon = 91.88$; $\zeta = 89.64$; $\eta = 80.20$; $\theta = 77.04$; $\kappa = 131.02$; $\lambda = 130.98$; $\mu = 129.18$; $\nu = 117.74$°.

at 4.299 Å. Exchange ($\mathcal{J}_2$) will be either "direct" or via the 4 Sb_{II} neighbors (2) which form with Eu a flat square pyramid, or via the Sb_I atoms on the other side (5). The 2 Eu neighbors along the a-axis are much more remote, namely at 4.768 Å. Exchange ($\mathcal{J}_3$) will take place via the same Sb_{II} atoms (3) with an Eu–Sb_{II}–Eu angle $\varepsilon = 91.88°$, or via the Sb_I atoms within the (a, c) plane (4) which are at angles $\zeta = 89.64°$ and $\eta = 80.20°$. Moreover, still within the same double layer, each Eu atom has 4 Eu neighbors in the other Eu layer (6). These are connected by two paths ($\mathcal{J}_4$) via an Sb_{II} atom at an angle $\kappa = 131.02°$ or at an angle $\lambda = 130.98°$. The indirect coupling between the slabs ($\mathcal{J}_5$, 7 in Fig. 4) is very similar to the foregoing. The Eu–Sb–Eu angles are $\mu = 129.18°$ and $\gamma = 117.74°$. The angles in (6) and (7) are somewhat closer to 180° and therefore more favorable for antiferromagnetic superexchange than in all the other Eu–Sb–Eu paths. Finally, the four diagonal neighbors within the flat-pyramid arrays in the (a, b) plane are coupled via superexchange at an Eu–Sb–Eu angle of 150.74° ($\mathcal{J}_6 < 0$). This antiferromagnetic exchange might favor the arrangement (a).

From the susceptibility measurements in the paramagnetic temperature range we derived $\theta_p \approx 0$ ($\theta_p = +2°K$ for the crystal with H ∥ (001), $\theta_p = -1°K$ for the crystal with $H \perp (001)$ and $\theta_p = -4°K$ for the crystal studied at high temperatures). Since $\theta_p \sim \mathcal{J}_p$, where

$$\mathcal{J}_p = 2\mathcal{J}_1 + 2\mathcal{J}_2 + 2\mathcal{J}_3 + 4\mathcal{J}_4 + 4\mathcal{J}_5 + 4\mathcal{J}_6 + \cdots,$$

we conclude that $\mathcal{J}_p \approx 0$. For the magnetic arrangements (b) and (c) the corresponding exchange parameters $\mathcal{J}_{af}$ are:

$$\mathcal{J}_{af}^{+-+-} = (2\mathcal{J}_2 + 2\mathcal{J}_3 + 4\mathcal{J}_6) - (2\mathcal{J}_1 + 4\mathcal{J}_4) - 4\mathcal{J}_5 + \cdots,$$

$$\mathcal{J}_{af}^{++--} = (2\mathcal{J}_2 + 2\mathcal{J}_3 + 4\mathcal{J}_6) + (2\mathcal{J}_1 + 4\mathcal{J}_4) - 4\mathcal{J}_5 + \cdots,$$

$$\mathcal{J}_{af}^{+--+} = (2\mathcal{J}_2 + 2\mathcal{J}_3 + 4\mathcal{J}_6) - (2\mathcal{J}_1 + 4\mathcal{J}_4) + 4\mathcal{J}_5 + \cdots.$$

Approximating $\mathcal{J}_p \approx 0$ leads to ($\mathcal{J}_{af} \approx 2\mathcal{J}_{\uparrow\downarrow}$):

$$\mathcal{J}_{af}^{+-+-} \approx -4\mathcal{J}_1 - 8\mathcal{J}_4 - 8\mathcal{J}_5 = \mathcal{J}_{af}^{++--} + \mathcal{J}_{af}^{+--+},$$

$$\mathcal{J}_{af}^{++--} \approx -8\mathcal{J}_5 = 8|\mathcal{J}_5|,$$

$$\mathcal{J}_{af}^{+--+} \approx -4\mathcal{J}_1 - 8\mathcal{J}_4 \overset{(?)}{=} 4|\mathcal{J}_1| + 8|\mathcal{J}_4|.$$

From the Eu–Sb–Eu angles in (6) and (7) we conclude that superexchange makes both $\mathcal{J}_4$ and $\mathcal{J}_5$ negative and probably $|\mathcal{J}_5| > |\mathcal{J}_4|$. It is very risky to extrapolate from the Eu chalcogenides where the coordination is different, but tentatively we assume $\mathcal{J}_1 > 0$. If, moreover, $\mathcal{J}_1 > 2\mathcal{J}_4$ then the ++ −− magnetic structure is realized; in the opposite case it is the totally antiferromagnetic arrangement +− +−. Unfortunately, we have no idea about the exchange contribution of the free electrons in our (possibility semimetallic) sample. If the differences between $\mathcal{J}_{af}^{+-+-}$ and $\mathcal{J}_{af}^{++--}$ are small enough, the magnetic arrangement might be influenced by partial anion substitution, and/or by a $CaSb_2$-type → $ZrSi_2$-type transition. For a detailed discussion one probably should also take the dipolar energy into account. Anyway, the final answer about the actual magnetic order has to be given by neutron diffraction.

Acknowledgments

We are highly indebted to Prof. G. Busch and Prof. D. Schwarzenbach for their stimulating interest and support. Moreover, we thank Mr. G. Burri for various electron-beam microanalyses and Dr. O. Vogt for the permission to use the moving-sample magnetometer. Financial support by the Swiss National Science Foundation is gratefully acknowledged.

References

1. G. Chapuis, F. Hulliger, and R. Schmelczer, to be published.
2. K. Deller and B. Eisenmann, *Z. Anorg. Allg. Chem.* **425**, 104 (1976).

3. K. DELLER AND B. EISENMANN, *Z. Naturforsch. B* **31**, 1146 (1976).
4. "The X-Ray System," Technical Report TR-192, Computer Science Center, University of Maryland (1972), modified by D. Schwarzenbach.
5. D. CROMER AND J. MANN, *Acta Crystallogr. A* **24**, 321 (1968).
6. D. CROMER, *Acta Crystallogr.* **18**, 17 (1965).
7. F. HULLIGER, *in* "Hdb. Physics and Chem. Rare Earths" (ed. K. A. Gschneider and L. Eyring, Eds.), Vol. **IV**, Chap. 2, North–Holland Amsterdam, (1979).
8. R. E. BODNAR, H. STEINFINK, AND K. S. V. L. NARASIMHAN, *J. Appl. Phys.* **39**, 1485 (1968).
9. J. NEUBUESER AND H. WONDRATSCHEK, "Maximal Subgroups of the Space Groups," University of Karlsruhe (1969).
10. G. SFEZ AND C. ADOLPHE, *Bull. Soc. Fr. Minéral. Cristallogr.* **95**, 553 (1972).
11. E. MOOSER AND W. B. PEARSON, *Phys. Rev.* **101**, 1608 (1956); *Progr. Semicond.* **5**, 103 (1960).
12. H. SCHÄFER, B. EISENMANN, AND W. MÜLLER, *Angew. Chem.* **85**, 742 (1973).